MONTE CARLO STUDY OF PHASE DIAGRAMS AND MAGNETIC PROPERTIES OF TRILAYER SUPERLATTICES

S. Naji[a,b], A. Belhaj[c], H. Labrim[d], L. Bahmad[a†]
A. Benyoussef[a,e,f], A. El Kenz[a]

[a]Laboratoire de Magnétisme et Physique des Hautes Énergies
(LMPHE-URAC 12) Faculté des Sciences, Université Mohammed V-Agdal
Rabat, Morocco
[b]Department of Physics, Faculty of Science, Ibb University, Ibb, Yemen
[c]Département de Physique, Faculté Polydisciplinaire, Université Sultan Moulay
Slimane Béni Mellal, Morocco
[d]Centre National de l'Energie, des Sciences et des Techniques Nucléaires
Rabat, Morocco
[e]Institute of Nanomaterials and Nanotechnology, MAScIR, Rabat, Morocco
[f]Hassan II Academy of Science and Technology, Rabat, Morocco

(Received November 18, 2013; revised version received January 17, 2014)

In this work, we build a superlattice Ising model based on periodic trilayers consisting of spin particles $\sigma = \frac{1}{2}$, $S = 1$ and $q = \frac{3}{2}$ placed at square lattice sites. More precisely, we study the effect of the inter-couplings $J_{\alpha\beta}(\alpha, \beta = \sigma, S, q)$ between the trilayers in the presence of an external magnetic field H. We first elaborate the ground state phase diagrams in the $(H, J_{\sigma S})$-plane. We find that the most stable phases are associated with the triplets $(\sigma, S, q) = ((-\frac{1}{2}, 1, \frac{3}{2}), (\frac{1}{2}, -1, -\frac{3}{2})\ (\frac{1}{2}, 1, \frac{3}{2}))$. For $J_{Sq} = -1$, three extra stable phases appear. In this case, seven different stable configurations arise. Then, we discuss the magnetic properties using Monte Carlo simulations. The thermal behaviors of the magnetizations and the susceptibilities are computed and discussed. For different temperatures, the magnetic field effect on the total magnetization has been investigated, leading to the hysteresis loops. Moreover, it has been found that the effect of the coupling interactions on the total magnetization controls the magnetic phase type, which can be either ferromagnetic or ferrimagnetic depending on the values of $J_{\alpha\beta}$ couplings.

DOI:10.5506/APhysPolB.45.947
PACS numbers: 75.10.Hk, 75.30.Kz, 75.30.Et, 77.80.–E

† Corresponding author: bahmad@fsr.ac.ma

1. Introduction

Over the last few decades, the elaboration of the magnetic materials has received a remarkable interest due to their high spin polarization considered as promising candidates for nanotechnology and spintronic applications [1–3]. Magnetic behaviors of various materials have been extensively investigated using different techniques including the mean field approximation (MFA) and Monte Carlo simulation [4, 5], effective-field theory [6], finite cluster approximation [7], renormalization group [8] and series expansions [9]. On the basis of these activities, many models relaying on planar superlattice engineering methods have been used to deal with the magnetic properties of multilayer systems using mean field method and Monte Carlo simulations [10, 11]. In fact, a particular interest has been devoted to study bilayer systems using alternating geometry [12].

Alternative activities on such materials have been made. In particular, the magnetic superlattices of doped materials have been built at nano-scale. For instance, the GaMnAs material has been obtained by layering GaAs and using Mn-impurity densities. More precisely, the static critical behavior of the magnetic material superlattices have been investigated, and the corresponding static critical exponents have been calculated by performing simulation methods [13, 14]. An other example concerns the perovskite $LaMnO_3$ which is considered as the parent of the negative colossal and tunnel magnetoresistance compounds. This model involves a magnetic structure with an alternate opposed spin layers [15]. Similar studies based on model Hamiltonians have been given in many places. In the framework of the Heisenberg model, the phase diagrams and the magnetic properties have been discussed using Monte Carlo simulations [16].

More recently, a special interest has been devoted to study trilayer systems successfully explored in spintronic device fabrications [17]. It has been found that one can find nice attractive magnetic properties in hole-doped Mn/Si trilayers [18]. Other models based on the graphene, relaying on the honeycomb structure, have been also realized using different approaches including numerical calculations [19, 20].

In particular, in one of our previous works using MFA, some magnetic properties of the trilayer system have been discussed, based on a square structure proposed in [10]. More precisely, we have computed the reduced critical temperature and the magnetic properties. However, as sake of completness and in order to get more accurate results, we perform Monte Carlo simulations to show the effect of magnetic field on phase diagrams and magnetic properties of such system.

The aim of this paper is to contribute to these activities by presenting a Monte Carlo study of a super-lattice Ising model based on periodic trilayers consisting of particles with spins $S = \frac{1}{2}$, $\sigma = 1$ and $q = \frac{3}{2}$ residing on the

sites of a square lattice. More precisely, we discuss the effect of the coupling interactions $J_{\alpha\beta}(\alpha, \beta = \sigma, S, q)$ between the trilayers in the presence of an external magnetic field H. We first investigate the ground state phase diagrams in the plane $(H, J_{\sigma S})$. It has been shown that the most stable phases are associated with the triplets $(\sigma, S, q) = ((-\frac{1}{2}, 1, \frac{3}{2}), (\frac{1}{2}, -1, -\frac{3}{2}) (\frac{1}{2}, 1, \frac{3}{2}))$. Three extra stable phases arise for $J_{Sq} = -1$ producing seven phase regions. Then, we study the corresponding magnetic properties using Monte Carlo simulations. The thermal behaviors of the magnetizations and the susceptibilities are calculated and investigated. For different temperatures, the magnetic field effect on the total magnetization has been discussed. We compute the hysteresis loops. We show that the effect of the coupling interactions, on the total magnetization, determines the type of the magnetic phase which can be either ferromagnetic or ferrimagnetic depending on the values of $J_{\alpha\beta}$.

2. The model

The model we study here is based on a trilayer superlattice consisting of Ising spins in the presence of an external magnetic field. It is formed by periodic trilayers of spins $\sigma = \frac{1}{2}$, $S = 1$ and $q = \frac{3}{2}$ living on square lattice sites. For later use, we refer to three layers as σ-layer, S-layer and q-layer, respectively. The geometry of this model is illustrated in Fig. 1. Its physical properties can be discussed in terms of the following Hamiltonian

$$\begin{aligned}\mathcal{H} \;=\; & -J_{\sigma\sigma}\sum_{(i,j)}\sigma_i\sigma_j - J_{SS}\sum_{(i,j)}S_iS_j - J_{qq}\sum_{(i,j)}q_iq_j \\ & -J_{\sigma S}\sum_{(i,j)}\sigma_iS_j - J_{\sigma q}\sum_{(i,j)}\sigma_iq_j - J_{Sq}\sum_{(i,j)}S_iq_j \\ & -H\sum_i(\sigma_i + S_i + q_i)\,. \end{aligned} \tag{1}$$

The notation (i, j) represents a pair of the nearest neighbor superlattice sites. $J_{\alpha\alpha}(\alpha = \sigma, S, q)$ denotes the coupling interactions between the particles living in the same layer (α-layer). The coupling $J_{\alpha\beta}(\alpha, \beta = \sigma, S, q)$ are associated with the interactions between particles belonging to two different layers(α-layer and β-layer). H is an external magnetic field which is applied normally on the layer planes.

Having built the corresponding Hamiltonian, the strategy in the rest of this paper is to perform Monte Carlo simulations to discuss the magnetic properties. The most important physical quantities will be calculated and discussed in the forthcoming sections.

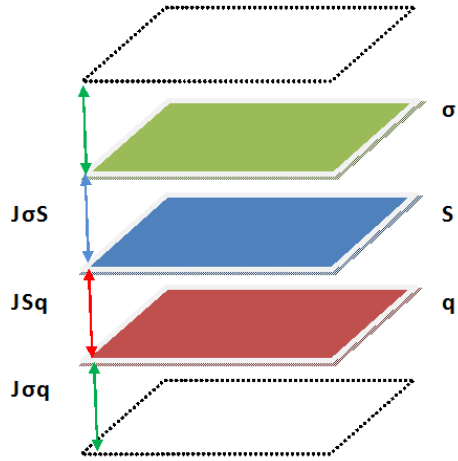

Fig. 1. The geometry of the trilayer superlattice.

3. Ground state phase diagrams

Before discussing the magnetic properties, we start first by an analytical examination of the ground state phase diagrams of the model described by the Hamiltonian (1). It is worth noting that the α-layer consists of L^2 spins placed on a superlattice with a square geometrical structure. The ground state phase diagrams can be obtained by computing and comparing all possible configuration energies. For the present model, the number of the possible configurations is $(2\sigma+1)\times(2S+1)\times(2q+1)=24$. It turns out that the calculation usually depends on the moduli space parameterized by the exchange coupling interactions $J_{\alpha\alpha}(\alpha=\sigma,S,q)$, $J_{\alpha\beta}(\alpha,\beta=\sigma,S,q)$ and the external magnetic field H. However, the general study is beyond the scope of the present work, though we will consider particular regions of the moduli space. In the present study, we fix the values of $J_{\alpha\alpha}=1$, while we vary the values of the external magnetic field H in terms of $J_{\sigma S}$ for special values of $J_{\sigma q}=\pm1$ and $J_{Sq}=\pm1$. The positive and the negative values correspond to ferromagnetic and antiferromagnetic interactions respectively. The corresponding ground state phase diagrams are determined analytically. In this way, the Hamiltonian (1) can produce four topologies formed by different phase diagrams. These topologies are classified in terms of the values of the couple $(J_{\sigma q},J_{Sq})$. Namely, the ferro–ferro topology FF, the antiferro–ferro topology AF, the ferro–antiferro topology FA and the antiferro–antiferro topology AA. For an organization reason, we list them in Table I.

TABLE I

A sketch of different topologies, for $J_{\sigma S} = 1$.

Topology	$J_{\sigma q}$	J_{Sq}
FF	1	1
AF	1	-1
FA	-1	1
AA	-1	-1

The corresponding phase diagrams are presented in Fig. 2. It follows from this figure that there are seven stable phases associated with the triplets (σ, S, q). Only four of them appear in all topologies. These four phases are given by the following triplets: $(-\frac{1}{2}, -1, -\frac{3}{2})$, $(-\frac{1}{2}, 1, \frac{3}{2})$, $(\frac{1}{2}, -1, -\frac{3}{2})$ and $(\frac{1}{2}, 1, \frac{3}{2})$. The complete picture is shown in Table II.

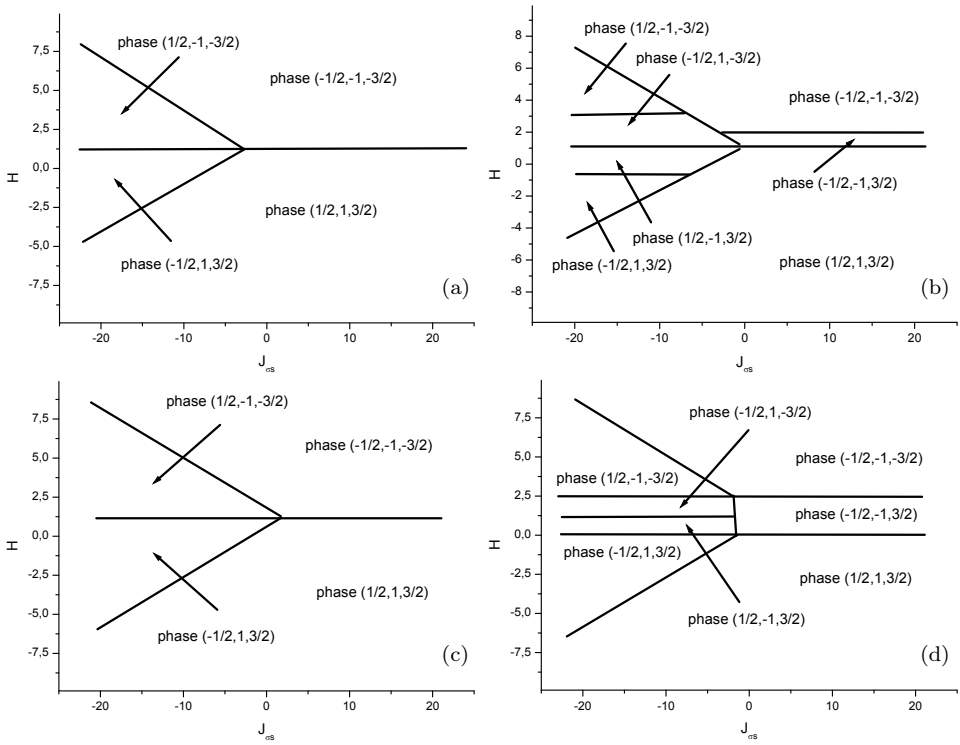

Fig. 2. The ground state phase diagrams.

TABLE II

Different ordering phases associated with each topology.

Topology / Ordering phases	$(-\frac{1}{2},-1,-\frac{3}{2})$	$(-\frac{1}{2},1,\frac{3}{2})$	$(\frac{1}{2},-1,-\frac{3}{2})$	$(\frac{1}{2},1,\frac{3}{2})$	$(-\frac{1}{2},-1,\frac{3}{2})$	$(-\frac{1}{2},1,-\frac{3}{2})$	$(\frac{1}{2},-1,\frac{3}{2})$
FF	×	×	×	×			
AF	×	×	×	×	×	×	×
FA	×	×	×	×			
AA	×	×	×	×	×	×	×

The FF and FA topologies involve the same four stable phases represented in Fig. 2 (a) and Fig. 2 (c) respectively. They are associated with $(-\frac{1}{2},-1,-\frac{3}{2})$, $(-\frac{1}{2},1,\frac{3}{2})$, $(\frac{1}{2},-1,-\frac{3}{2})$ and $(\frac{1}{2},1,\frac{3}{2})$. The distribution of these four stable phases depends on the values of $J_{\sigma S}$. It follows from Fig. 2 (a) that for $J_{\sigma S} \geq -2$ it appears only two symmetrical phases $((-\frac{1}{2},1,\frac{3}{2})$, $(\frac{1}{2},-1,-\frac{3}{2})$ $(\frac{1}{2},1,\frac{3}{2}))$, while for $J_{\sigma S} \leq -2$, we have the four stable phases. Similar interpretation can be elaborated for the FA topology. However, the difference can be seen at the level of the location of the critical points and the size of the phase regions.

The same phenomena arises in AF and AA topologies shown in Fig. 2 (b) and Fig. 2 (d) respectively. These topologies have, however, seven stable phases associated with the triplets $(-\frac{1}{2},-1,-\frac{3}{2})$, $(-\frac{1}{2},1,\frac{3}{2})$, $(\frac{1}{2},-1,-\frac{3}{2})$, $(\frac{1}{2},1,\frac{3}{2})$, $(-\frac{1}{2},1,\frac{3}{2})$, $(-\frac{1}{2},1,\frac{3}{2})$, $(\frac{1}{2},1,\frac{3}{2})$. As the previous topologies, the distribution of these seven stable phases depends on the values of $J_{\sigma S}$ couplings. The difference between these topologies comes essentially from the size phases and theirs intersection locations. These two topologies have more stable phases then they appear to be more interesting from the physical point of view.

4. Monte Carlo study: results and discussions

In this section, we study the phase diagrams and the magnetic properties of the proposed model using Monte Carlo simulations. In particular, we perform a Monte Carlo study to deal with the Hamiltonian (1) associated with the geometry illustrated in Fig. 1. The analysis will be based on the boundary periodic conditions, 10^5 Monte Carlo steps for each spin configuration and discarding the first 10^4 generated configurations. Preliminary calculations are performed for various system sizes namely $L = 16,\ 24,\ 32$ and 64. In what follows, the system size L will be fixed to 32 spins in each direction.

Averaging over many configurations, we compute the most important physical quantities. Indeed, we first calculate the partial and total magnetizations per site

$$
\begin{aligned}
M_\sigma &= \frac{1}{L^2}\left\langle \sum_i \sigma_i \right\rangle , \\
M_S &= \frac{1}{L^2}\left\langle \sum_i S_i \right\rangle , \\
M_q &= \frac{1}{L^2}\left\langle \sum_i q_i \right\rangle , \\
M_t &= \frac{1}{3}\left(M_\sigma + M_S + M_q\right) . \qquad (2)
\end{aligned}
$$

Then, we compute the partial and total magnetic susceptibilities

$$
\begin{aligned}
\chi_\sigma &= \frac{1}{k_\beta T}\left(\langle M_\sigma^2\rangle - \langle M_\sigma\rangle^2\right) , \\
\chi_S &= \frac{1}{k_\beta T}\left(\langle M_S^2\rangle - \langle M_S\rangle^2\right) , \\
\chi_q &= \frac{1}{k_\beta T}\left(\langle M_q^2\rangle - \langle M_q\rangle^2\right) , \\
\chi_t &= \frac{1}{k_\beta T}\left(\langle M_t^2\rangle - \langle M_t\rangle^2\right) , \qquad (3)
\end{aligned}
$$

where T is the absolute temperature. k_β is the Boltzmann constant which will be fixed to the unit value.

In this Monte Carlo study, we restrict ourselves to the triplet $(\sigma, S, q) = (\frac{1}{2}, 1, \frac{3}{2})$ belonging to the FF topology (Fig. 2 (a)). In Fig. 3 (a), (b), (c), we plot the thermal behaviors of the partial magnetizations as well as the corresponding susceptibilities. It follows that at very low temperature values, the partial magnetizations reach their maximum values, which is in good agreement with the ground state phase diagram (see Fig. 2 (a)). Moreover, the critical temperature corresponds to a peak as it is shown in the susceptibility curves. We expect that the same behavior could appear in the total magnetization and the susceptibility.

In order to study the effect of the external magnetic field H, we plot in Fig. 4 the total magnetization in terms of H for specific values of the temperature ($T = 1K$, $T = 2K$, $T = 3K$ and $T = 4K$). The total curve magnetization exhibits hysteresis loops. It is found that the increasing of the magnetic field effect decreases the total magnetization. It is worth noting that this behavior is observed for the above temperatures. When the temperature increases (decreases), for a fixed value of the external magnetic field, the total magnetization decreases (increases).

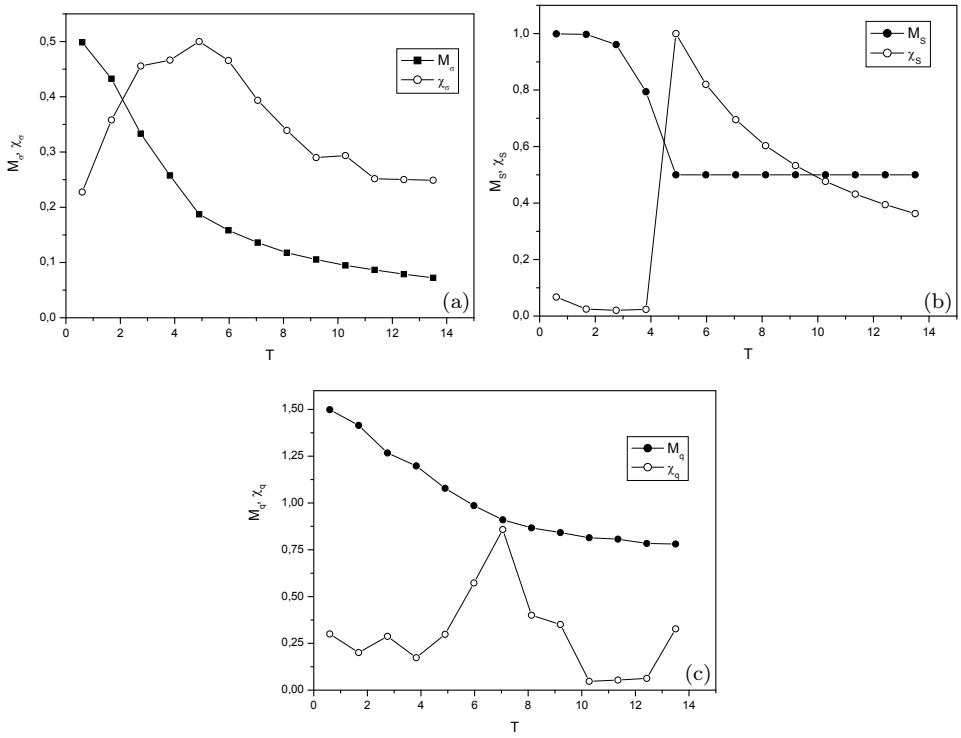

Fig. 3. The partial magnetizations and susceptibilities as a function of the reduced temperature.

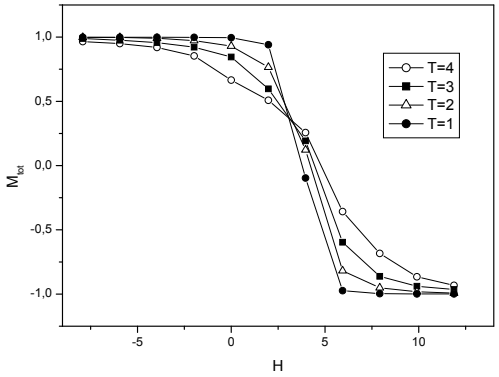

Fig. 4. The total magnetization in terms of the external magnetic field H for specific values of the reduced temperature ($T = 1$, $T = 2$, $T = 3$ and $T = 4$).

To discuss the effect of the coupling interactions on the system, we present in Fig. 5 (a), (b), (c) the total magnetization in terms of $J_{\alpha\beta}(\alpha, \beta = \sigma, S, q)$ for specific values of the temperature ($T = 1K$, $T = 2K$, $T = 3K$ and $T = 4K$). For all temperatures, it is found that the increasing of $J_{\alpha\beta}$ increases the total magnetization. For a fixed value of $J_{\alpha\beta}$, the total magnetization decreases when one increases the temperature. Comparing the behavior of the total magnetizations, it is observed that there are two regions: large positive values of $J_{\alpha\beta}$ and large negative values of $J_{\alpha\beta}$. In the first region, the ferromagnetic phase $(\sigma, S, q) = (\frac{1}{2}, 1, \frac{3}{2})$ is the most stable. However, in the second region, the most stable magnetic phases depend on the $J_{\alpha\beta}$ coupling interactions. Indeed, these stable phases can be either antiferromagnetic for J_{Sq} or ferrimagnetic for the remaining ones.

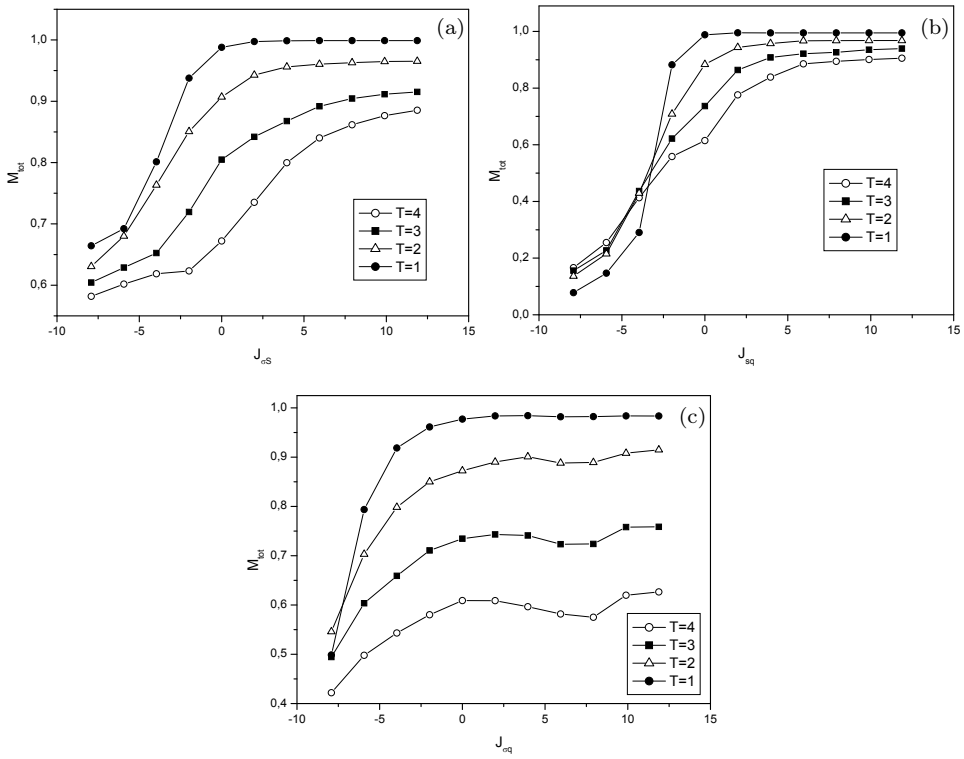

Fig. 5. The total magnetizations as a function of $J_{\alpha\beta}(\alpha, \beta = \sigma, S, q)$ for specific values of the reduced temperature ($T = 1$, $T = 2$, $T = 3$ and $T = 4$).

5. Conclusion

In this paper, the phase diagrams and magnetic properties of trilayer superlattices have been investigated using Monte Carlo study. The model is based on a trilayer superlattice consisting of particles with spins $\sigma = \frac{1}{2}$, $S = 1$ and $q = \frac{3}{2}$, residing on the sites of a square lattice. In particular, we have investigated the effect of the coupling interactions $J_{\alpha\beta}(\alpha, \beta = \sigma, S, q)$ between the trilayers in the presence of an external field H. We have given the ground state phase diagrams in the plane (H, $J_{\sigma S}$). We have shown that the most stable phases are associated with the triplets $(\sigma, S, q) = ((-\frac{1}{2}, 1, \frac{3}{2}), (\frac{1}{2}, -1, -\frac{3}{2})\ (\frac{1}{2}, 1, \frac{3}{2}))$. Three additional configurations arise for $J_{Sq} = -1$. Then, we have studied the magnetic properties using Monte Carlo simulations. The thermal behaviors of the magnetizations and the susceptibilities have been calculated and discussed. For different temperatures, the magnetic field effect on the total magnetization has been investigated. The hysteresis loops have been found and discussed. Among others, it has been revealed that the effect of the coupling interactions, on the total magnetization, determines the magnetic phase type which can be either ferromagnetic or ferrimagnetic depending on the values of $J_{\alpha\beta}$.

REFERENCES

[1] T. Dietl *et al.*, *Science* **287**, 1019 (2000).

[2] T. Dietl, *Nature Mater.* **9**, 965 (2010).

[3] D. Gatteschi, O. Kahn, J.S. Miller, F. Palacio (Eds.), *Magnetic Molecular Materials*, NATO ASI E **198**, Plenum (1991).

[4] P. Weiss, *J. Phys. Radium* **6**, 661 (1907); H.E. Stanley, *Introduction to Phase Transitions and Gitical Phenomena*, Oxford University Press, 1971; M. Yeomans, *Statistical Mechanics of Phase Transitions*, Oxford 1993.

[5] K. Binder, P.C. Hohenberg, *Phys. Rev.* **B9**, 2194 (1974); K. Binder, D.W. Heermann, *Monte Carlo Simulation in Statistical Physics: An Introduction*, Springer Series in Solid-state Sciences (2002).

[6] R. Honmura, T. Kaneyoshi, *J. Phys. C Solid State Phys.* **12**, 3979 (1979).

[7] N. Boccara, *Phys. Lett.* **A94**, 185 (1983); A. Benyoussef, N. Boccara, *J. Appl. Phys.* **55**, 1667 (1985).

[8] K.G. Wilson, *Phys. Rev.* **B4**, 3184 (1971).

[9] J. Oitmaa, *Phys. Lett.* **A33**, 230 (1970).

[10] S. Naji *et al.*, *Physica A* **399**, 106 (2014).

[11] O.D.R. Salmona *et al.*, *Phys. Lett.* **A377**, 1991 (2013).

[12] M. El Yadari, L. Bahmad, A. El Kenz, A. Benyoussef, *Physica A* **392**, 673 (2013).

[13] A. Koeder *et al.*, *Appl. Phys. Lett.* **85**, 783 (2004) [arXiv:cond-mat/0308618 [cond-mat.mtrl-sci]].

[14] J. Sadowski *et al.*, arXiv:1201.2166 [cond-mat.mtrl-sci].

[15] F. Moussa *et al.*, *Phys. Rev.* **B54**, 15149 (1996).

[16] S. Naji *et al.*, *Physica A* **391**, 3885 (2012).

[17] N.D. Sharma, C.M. Landis, P. Sharma, arXiv:1003.2745 [cond-mat.mes-hall].

[18] L.H. Yang *et al.*, *J. Phys. D Appl. Phys.* **46**, 165502 (2013).

[19] M. Serbyn, D.A. Abanin, *Phys. Rev.* **B87**, 115422 (2013).

[20] C.H. Lui *et al.*, *Nature Phys.* **7**, 944 (2011).